


Article

Interaction of Si Atom with the (001) Surface of TiN, AlN and TaN Compounds

Leonid Svyatkin ^{1,*} , Sergey Ognev ^{1,2}, Maxim Syrtanov ¹ and Yury Koroteev ²
¹ Division for Experimental Physics, National Research Tomsk Polytechnic University, 634050 Tomsk, Russia; soo1@tpu.ru (S.O.); mss12@tpu.ru (M.S.)

² Institute of Strength Physics and Materials Science of Siberian Branch Russian Academy of Sciences, 634055 Tomsk, Russia; koroteev@ispms.tsc.ru

* Correspondence: svyatkin@tpu.ru

Abstract: Nowadays, the application of multicomponent coatings with multiphase nanocrystalline structure is the most promising direction in the search for wear-resistant protective coatings with a full set of necessary operational properties. Nanocrystalline multicomponent coatings based on the Ti–Al–Ta–Si–N system have a high hardness combined with thermal stability and oxidation resistance. Silicon atoms are weakly soluble in the TiN, $Ti_{1-x}Al_xN$, and TaN crystalline phases of the Ti–Al–Ta–Si–N system and interact preferentially with N atoms, forming the amorphous Si_3N_4 phase. In this context, it is important to first study the peculiarities of the interaction of Si atoms with the simplest structural units of the Ti–Al–Ta–Si–N system, such as TiN, AlN, and TaN compounds with the NaCl structure. This work is devoted to the study of the interaction of a Si atom with the (001) surface of AlN, TiN, and TaN compounds with the NaCl structure using ab initio calculations. This provides information for a deep understanding of the initial stages of the formation of different crystallites of the considered composite. It was established that the adsorption of silicon on the (001) surface of AlN, TiN, and TaN significantly increases the relaxation of the surface layers and leads to an increase in the corrugation observed on the clean surfaces. The largest corrugation is observed on the surface of the TaN compound. The most energetically favorable adsorption positions of Si atoms were found to be the position of Si above the N atom on the TiN and TaN surfaces and the quadruple coordinated position on the AlN surface. The valence electron density distribution and the crystal orbital Hamiltonian population were studied to identify the type of Si atom bonding with the (001) surface of AlN, TiN, and TaN compounds. It was found that silicon forms predominantly covalent bonds with the nearest metal and nitrogen atoms, except for the quadruple coordinated position on the surface of TiN and TaN, where there is a high degree of ionic bonding of silicon with surface atoms.

Keywords: silicon; surface; atomic structure; charge transfer; density of states



Citation: Svyatkin, L.; Ognev, S.; Syrtanov, M.; Koroteev, Y. Interaction of Si Atom with the (001) Surface of TiN, AlN and TaN Compounds. *Coatings* **2023**, *13*, 1453. <https://doi.org/10.3390/coatings13081453>

Academic Editor: Alberto Palmero

Received: 8 July 2023

Revised: 14 August 2023

Accepted: 15 August 2023

Published: 17 August 2023



Copyright: © 2023 by the authors. Licensee MDPI, Basel, Switzerland. This article is an open access article distributed under the terms and conditions of the Creative Commons Attribution (CC BY) license (<https://creativecommons.org/licenses/by/4.0/>).

1. Introduction

The application of wear-resistant protective coatings is one of the most promising methods to improve the functional properties of contacting materials, thus effectively solving the problems of friction and wear. Nanocrystalline multicomponent coatings based on Ti–Al–N solid solution are known to exhibit a high hardness combined with thermal stability and oxidation resistance [1,2]. One way to improve the performance characteristics of Ti–Al–N solid solution is to simultaneously introduce an impurity of Ta and Si into its composition. Tantalum increases crack resistance, heat resistance, and oxidation resistance [3,4], and silicon interacting with nitrogen leads to the formation of a nanocrystalline structure and increases hardness [5,6]. The experimental study of the microstructure of TiN coatings following the metal vapor vacuum arc plasma ion implantation of Si ions at different ion doses reveals the formation of amorphous Si_3N_4

phase within the implantation matrix of the TiN coatings [7]. The same result was observed in the Ti-Al-Si-N [5] and Ta-Si-N [8] coatings: Si atoms interact preferentially with N atoms forming Si_3N_4 and are found in small amounts in the crystalline TiN, $\text{Ti}_{1-x}\text{Al}_x\text{N}$ and TaN phases. This is due to the poor solubility of silicon in the considered metal nitrides and leads to the formation of Si_3N_4 films on the boundaries of the crystallites, inhibiting their growth. Thus, a fine-grain structure of the nanostructured composite coatings is formed, which increases their resistance to brittle fracture. The ab initio study [9] of the $\text{Ti}_{1-x-y}\text{Si}_x\text{Al}_y\text{N}$ solid solution revealed that the alloying of TiN with Si and Al causes a general decrease in elastic constant, cohesive and formation energies due to the weakening of the Ti-N bond. The ab initio study of the chemical bonds in bulk TiN and TiN-based $\text{Ti}_{1-x}\text{Al}_x\text{N}$ and $\text{Ti}_{1-x-y}\text{Al}_x\text{Ta}_y\text{N}$ solid solutions [10] revealed the role of Ti, Al, and Ta in the mechanical properties of the Ti-Al-Ta-N composite. These are good examples of using the ab initio study of the interaction between the atoms of the composite to explain the physical properties of coatings.

Current experimental techniques for obtaining new multicomponent coatings are mainly based on the sequential selection of elements of the periodic system as alloying components of the Ti-Al-N base to identify the configuration of a multicomponent alloy with the desired set of physical and mechanical properties. On the other hand, this task can be significantly accelerated by a targeted search for a multi-component alloy with the desired properties based on first-principles calculations. Given the important role of the formation of the amorphous Si_3N_4 phase in the Ti-Al-Ta-Si-N system, the question arises as to the nature of the interaction of the silicon atom with the metal and nitrogen atoms in the system. To date, no work has been devoted to the study of the atomic and electronic structure of components of nanostructured protective coatings based on the Ti-Al-Ta-Si-N system. The study of the behavior of Si atoms on the $\text{Ti}_{1-x-y}\text{Al}_x\text{Ta}_y\text{N}$ surface reveals the nature of the mechanical properties and structural phase stability of the Ti-Al-Ta-Si-N composite. This is important in the search for the optimal composition of multicomponent coatings with enhanced characteristics. First of all, it seems important to study the features of the interaction between Si atoms and the simplest structural units of the Ti-Al-Ta-Si-N system such as TiN, AlN, and TaN compounds. This provides information that is lacking in the literature for a deep understanding of the initial stages of formation of different crystallites of the considered composite. TiN coatings are characterized by the preferred orientation of the (200) planes [7]. In this regard, the study of the behavior of silicon on the (001) surface of TiN, AlN, and TaN compounds seems to be reasonable and a priority. The effect of Si atoms on the grain- and interface-formation mechanism during the deposition of the Ti-Si-N and Ta-Si-N nanocomposite films was studied in [11,12] using first-principles calculations. The energetic stability and configuration evolution behavior of the Ti-Si-N and Ta-Si-N islands on the (001) surface of TiN and TaN with the NaCl structure, respectively, were investigated. It was shown that the most stable configuration of Ti-Si-N and Ta-Si-N islands is obtained when the metal and nitrogen atoms combine to form islands and the silicon atoms remain outside these islands. In addition, the binding strength of the Si-Ti and Si-Ta bonds is found to be greater than that of the Si-N bond in the considered islands. However, the detailed analysis of the nature of the interaction of Si with the TiN(001), AlN(001), and TaN(001) surfaces is lacking in the literature. In this regard, the present work is devoted to the first-principles study of the influence of silicon adsorption on the atomic and electronic structures of the (001) surface of TiN, AlN, and TaN compounds with the NaCl structure and to the revealing of the features of interaction of silicon with the surface metal and nitrogen atoms of these compounds. The analysis of the valence electron distribution and density of electron states on the TiN(001), AlN(001), and TaN(001) surfaces with adsorbed Si atom allows for the identification of the character of the bonds between Si and surface N, Ti, Al, and Ta atoms.

2. Calculation Methods and Details

The ab initio calculations were performed using the plane-wave-based DFT ABINIT 8.6.1 software package [13,14]. The calculations were performed using a projector augmented wave (PAW) method, which is used to describe the electron-ion interaction [15,16]. The exchange and correlation effects were taken into account by the generalized gradient approximation proposed by Perdew, Burke, and Ernzerhof [17]. The integration in the Brillouin zone was performed on a special k-point mesh determined according to the Monkhorst-Pack scheme: $10 \times 10 \times 10$ for bulk calculations and $7 \times 7 \times 1$ for film calculations. The cut-off energy for the plane wave basis was set at 408 eV. The electron density self-consistency process was considered complete when the root mean square deviation of the output valence electron charge density from its input value became less than 10^{-3} electron·Å⁻³, corresponding to a total energy convergence no worse than 10^{-6} eV.

The lattice parameters of bulk AlN, TiN, and TaN compounds with the NaCl structure calculated by total energy minimization are presented in Table 1. Our values are in good agreement with previous calculations [12,18–21] and experimental results [22–26]. To study the interaction of silicon with the (001) surface of the TiN, AlN, and TaN compounds, a five-layer film in the 2×2 structure (see Figure 1) was used. As shown in Figure 1, each atomic layer in the supercell contains 4 metal atoms and 4 nitrogen atoms. A silicon atom was placed on only one surface of this film and was located in four symmetrical positions (Figure 1) on the MeN(001) surface: one bridge, two top positions and one quadruple coordinated (Q) position. In this case, the distance between Si atoms is ~6 Å and the interaction between them is negligible. This allows us to claim that we are studying the interaction of a single Si atom with the surface atoms of the considered compounds. The vacuum width was three lattice parameters: 12.78 Å, 12.20 Å, and 13.13 Å for TiN, AlN, and TaN, respectively. Optimization of the lattice parameters and relaxation of the atomic positions were performed using the Broyden-Fletcher-Goldfarb-Shanno algorithm. Relaxation of the atomic positions on the surface was carried out for three surface atomic layers below the adsorbed silicon atom and was considered complete when the force at each atom was less than $10 \text{ meV} \cdot \text{Å}^{-1}$. The two layers of the film on its clear side were fixed as in a bulk.

Table 1. The lattice parameter (in Å) of the bulk AlN, TiN, and TaN compounds with the NaCl structure.

Compound	This Work	Other Calculation	Experimental Results
AlN	4.061	4.016 [18]	4.043 [22]
TiN	4.237	4.265 [19]	4.244 [23]
		4.250 [20]	4.210 [24]
		4.258 [21]	4.243 [25]
TaN	4.389	4.403 [12]	4.310 [25]
			4.335 [26]

To analyze the nature of the Si-surface interaction, the valence electron distribution was studied and the Bader charge transfer [27] was calculated. The Crystal Orbital Hamiltonian Population (COHP) analysis [28] was used to study the effect of silicon on the interatomic chemical bonds at the (001) surface of the compounds considered. This technique is used for plane-wave electronic structure calculations (projected COHP) [29,30] and is implemented in the Local Orbital Basis Suite Towards Electronic-Structure Reconstruction (LOBSTER) code [31]. It allows energy-resolved local bonding analysis and splits the band structure energy into bonding and antibonding contributions from PAW electronic-structure calculations.

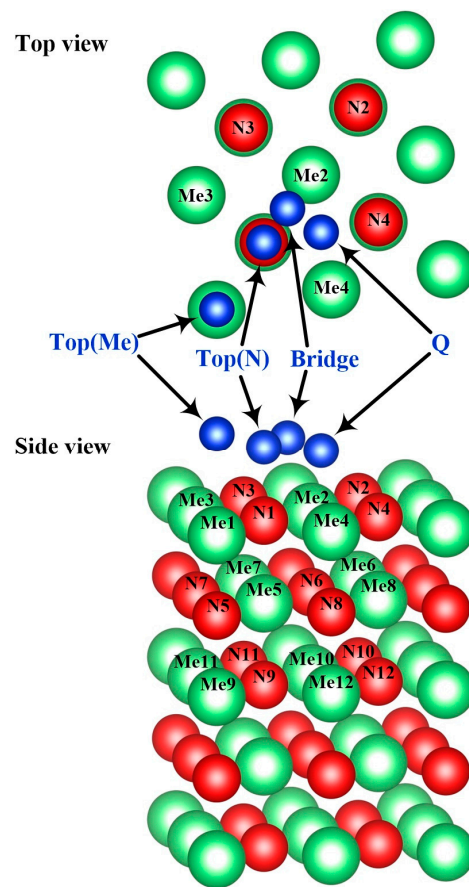


Figure 1. Top view and side view of the MeN(001) film with a Si atom adsorbed on a surface. The adsorption positions of the Si atom are marked by blue spheres. The green and red spheres are metal and nitrogen atoms, respectively.

3. Results and Discussion

3.1. Surface Atomic Structure

To analyze the stability of the surfaces considered, the surface energy was calculated by the formula

$$E_s = (E_{\text{film}} - E_{\text{bulk}})/2S \quad (1)$$

where E_{film} and E_{bulk} are the total energies of the film and bulk with the same number of atoms, and S is the surface area of the film. The factor of 2 accounts for the two equal surfaces in the film calculation.

It was found that the surface energy E_s of the bulk truncated AlN(001), TiN(001), TaN(001) surfaces are 96.1, 93.3, and 81.5 meV/Å², respectively. The surface relaxation reduces these values to 93.9, 83.5, and 57.1 meV/Å², respectively. Our results for AlN are about 9% higher than the calculated values given in [32,33] (85 meV/Å² and 83 meV/Å², respectively). For TiN, our results are approximately in the middle of the wide range of values from 77 to 109 meV/Å² given in [20,34–39]. For the metastable NaCl (B1) structure TaN(001) film, we unfortunately could not find any information about its surface energy.

Analyzing the results obtained, we can see that the smallest influence of surface relaxation is observed for AlN (2.2 meV/Å²) and the largest for TaN (24.4 meV/Å²). As can be seen in Figure 2 below, this can be explained by the fact that the AlN(001) surface has the smallest relaxation and the TaN(001) surface has the largest relaxation among the compounds considered. The lowest surface energies are observed for TaN, so the presence of tantalum atoms in the Ti-Al-Ta-N composite contributes to the viscous type of its fracture. The highest surface energy is observed for AlN, indicating the low probability of its surface formation, the high strength of the compound and its low plastic properties.

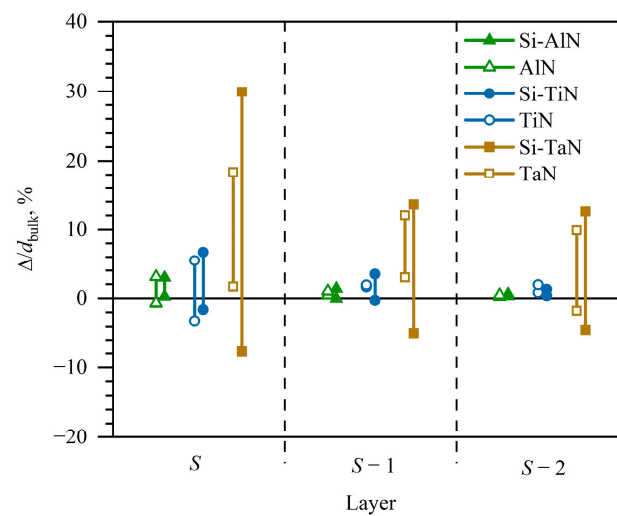


Figure 2. Relative displacement Δ/d_{bulk} of atoms in the surface and two subsurface layers along the surface normal. In the Si-MeN systems, the Si atom is adsorbed in the Top(N) position on the MeN surface. The segment length corresponds to the layer thickness δ_i and the segment center indicates the layer displacement z_i .

In the case where the atomic layers of the film are flat, the interplanar distances d_{ij} are simply defined as the difference between the z coordinates of the corresponding layer $d_{ij} = z_i - z_j$. The corrugation of the substrate surface layers complicates the situation by introducing an atomic structure characteristic as the layer thickness δ_i . There are several approaches to describe such a complex atomic structure [40,41]. In this paper, we use the approach applied in [40]. In particular, each atomic layer undergoing the corrugation is characterized by the layer thickness δ_i and the z_i coordinate of the layer center, calculated as the average of the largest and smallest z coordinates of the atoms in the layer. We calculated the displacement of the atom Δ from its ideal lattice position due to the relaxation at the surface (S) and subsurface ($S - 1$), ($S - 2$) layers:

$$\Delta = z - z_0, \quad (2)$$

where z and z_0 are the coordinates of the atoms along the axis perpendicular to the surface in the relaxed and unrelaxed films, respectively. To facilitate the comparison of the relaxation effect on the surface of the different compounds, this displacement Δ was related to the bulk value of the interplanar distance d_{bulk} , which is equal to half the lattice parameter of the considered compound. The largest and smallest atomic displacements Δ/d_{bulk} in the MeN(001) films are shown in Figure 3. In addition, the Δ/d_{bulk} values for the Si-MeN(001) films are also presented to show the effect of silicon adsorption in the Top(N) position on the surface relaxation.

The significant corrugation of the surface layers is observed on the clean (001) surface of TiN and TaN. The relative surface layer thickness δ_S/d_{bulk} is 8.7% and 16.7% for these compounds, respectively. The value of δ_S/d_{bulk} for AlN is significantly lower (3.8%). The surface layer displacement z_S/d_{bulk} reaches its maximum in TaN (10.0%) and minimum in AlN (1.2%). The relaxation decreases rapidly into the bulk of the AlN and TiN crystals: in the third layer from the surface, $\delta_{S-2}/d_{\text{bulk}}$ and z_{S-2}/d_{bulk} do not exceed 1.1% and 1.4%, respectively, whereas on the TaN surface, even in the third layer from the surface, $\delta_{S-2}/d_{\text{bulk}}$ and z_{S-2}/d_{bulk} are equal to 11.7% and 4.1%, respectively. The calculated values of the displacement and thickness of the surface layer are in good agreement with the results of other works [42–44], where the clean (001) surface of the TiN compound was studied. Silicon adsorption in the Top(N) position leads to an increase in the corrugation. The largest corrugation is observed on the surface of TaN: the relative layer thickness δ_i/d_{bulk} reaches 37.6% and the layer displacement z_i/d_{bulk} reaches 11.1%. The smallest

influence of silicon adsorption on the surface relaxation is observed on the surface of the AlN compound. The same results are observed for the other Si adsorption position considered on the (001) surface: the surface relaxation value varies slightly depending on the silicon adsorption position, but the general trend noted above remains. Increasing the surface corrugation can lead to an improvement in the adhesion properties of the surface by increasing the number of adsorption positions. This can be important when considering the non-equilibrium processes of sputtering a multi-component coating and the formation of its different crystalline phases.

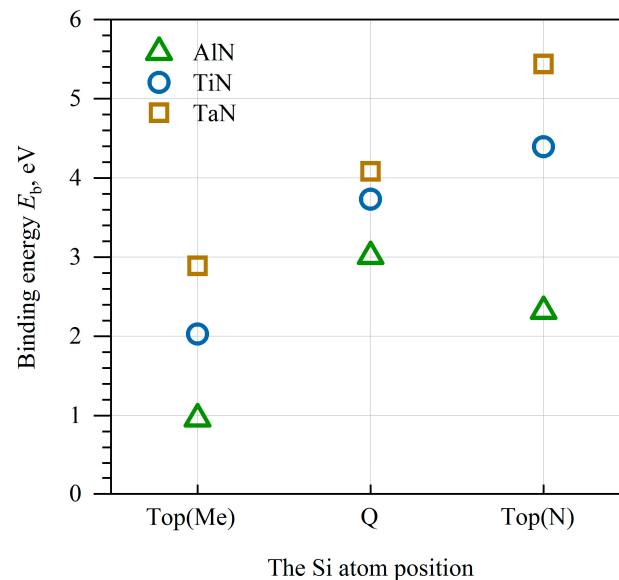


Figure 3. Binding energy E_b of silicon on the (001) surface of AlN, TiN, and TaN compounds.

3.2. Binding Energy

To describe the nature of the interaction of the silicon atom with the (001) surface for the different adsorption positions, its binding energy was calculated as

$$E_b = E(\text{Si}) + E(\text{MeN}) - E(\text{Si-MeN}) \quad (3)$$

where $E(\text{Si})$, $E(\text{MeN})$, and $E(\text{Si-MeN})$ are the total energies of the silicon atom and the supercell of the MeN and Si-MeN films, respectively. The binding energy is the minimum energy required to release a Si atom from the surface of the MeN system. When this value is positive, it is a quantitative characterization of the Si-MeN bond strength. The results of the calculations are presented in Figure 3. The binding energies of the silicon atom in the Bridge position are not shown because this position is unstable for all surfaces considered: the silicon atom is shifted to the nearest Top(N) position by relaxation.

The adsorption of silicon on the (001) surface of the AlN, TiN, and TaN compounds is characterized by a positive binding energy varying from 0.96 to 5.44 eV. On the TaN(001) surface, silicon is found to have the maximum binding energy, while on the AlN(001) surface, it has the lowest. The Top(N) position of Si is most energetically favorable on the TiN(001) and TaN(001) surfaces. In the case of the AlN(001) surface, the Q position is most energetically favorable. Figure 3 shows that the Si-Al bond is the weakest of the bonds considered.

To assess the validity and accuracy of the results presented, the effect of k-point sampling, cut-off energy and film thickness on the binding energy was studied. Increasing the special k-point mesh from $10 \times 10 \times 10$ to $20 \times 20 \times 20$ for bulk calculations and from $7 \times 7 \times 1$ to $14 \times 14 \times 1$ for film calculations changes the value of the Si binding energy by a value not exceeding 0.01 eV on the AlN and TaN surface and 0.05 eV on the TiN surface. The stronger influence of the k-point sampling on the binding energy of silicon on the surface of TiN compared to the other considered compounds indicates a stronger

inhomogeneity of the electron density in this compound. Increasing the cut-off energy for the plane-wave basis from 408 to 626 eV changes the value of the Si binding energy by an amount not exceeding 0.02 eV in all cases considered. In the third test, the film thickness was increased from five to nine layers. The relaxation of atomic positions on the surface of the thicker film was performed for four surface atomic layers below the adsorbed silicon atom. Increasing the film thickness results in a change in the silicon binding energy by no more than 0.04 eV on the AlN and TiN surfaces and an increase of ~ 0.4 eV on the TaN surface. The more significant effect of film thickness on the silicon binding energy on the TaN surface is due to the strong relaxation and corrugation of the surface of this compound. However, the need to correct for the large thickness of the TaN(001)-Si film does not qualitatively change the results shown in Figure 3, since it increases the binding energies of silicon on this surface. Thus, the chosen calculation parameters allow a fairly accurate description of the interaction of silicon with the (001) surface of the compounds under consideration.

3.3. Charge Density Distribution

To study the nature of the chemical bonding between silicon, metal and nitrogen atoms, the valence electron density distribution was analyzed. Figure 4 shows the results for both clean surfaces and surfaces with silicon atoms adsorbed in different positions. A mainly ionic type of bonding is observed between the Al and N atoms of AlN: the electron density is less than 0.01 electrons/ \AA^3 in the region of the Al atoms and more than 0.05 electrons/ \AA^3 in the vicinity of the N atoms (see the pink and yellow isosurfaces, respectively, around these atoms in Figure 4a). Since the Al and N atoms have 3 and 5 valence electrons, respectively, the observed difference in electron density in the vicinity of these atoms indicates the significant charge transfer from the Al atoms to the N atoms. The Si atom adsorbed on the surface AlN compound forms covalent bonds with the nearest Al and N atoms: the high density region is observed between the silicon atom and the nearest surface atom (see Figure 4a). The low density regions (~ 0.02 electrons/ \AA^3) are present in the interstitial of the AlN compound. The adsorption of Si atoms increases the size of these low-density regions near the surface. The largest increase in the size of these regions occurs with the adsorption of silicon in the Q position. This indicates an increase in the ion-covalent component of the Al-N bonds in the surface layers.

In the TiN compound, the ion-covalent bond is predominant: the yellow isosurfaces corresponding to the high valence electron density (0.05 electrons/ \AA^3 and more) surround the Ti and N atoms, and the size of this high-electron-density region is significantly larger in the vicinity of the N atoms than in the vicinity of the Ti atoms (see yellow isosurfaces around these atoms in Figure 4b), despite the close number of valence electrons in the Ti and N atoms (four and five electrons, respectively). As in the case of the AlN(001) surface, the silicon atom adsorbed on the TiN(001) surface forms covalent bonds with the nearest atoms. The electron density distribution in the vicinity of the silicon atom and the nearest surface atoms on the TiN surface (Figure 4b) is similar to that observed on the AlN surface (Figure 4a). In the interstitial of the TiN compound, the electron density is less than 0.02 electrons/ \AA^3 (these regions are bounded by the gray isosurfaces in Figure 4b). These low-density regions are absent between the first and second atomic layers. Silicon adsorption leads to the appearance of these low-electron-density regions in the surface layers and increases the size of the high-electron-density region between the Ti and N atoms. This indicates an increase in the covalent component of the Ti-N bonds in the surface layers.

In the case of TaN, the covalent-metal type of the Ta-N bond is observed: the regions with electron density below 0.02 electrons/ \AA^3 are present only between the second and third atomic layers (these regions occur due to the significant corrugation of the surface layer); the electron density in the interstitial region of the TaN compound is quite high (Figure 4c). The electron density distribution in the vicinity of the adsorbed silicon atom and the nearest surface atoms on the TaN surface is the same as on the AlN and TiN surfaces. Silicon adsorption in the Top(N) position on the TaN surface leads to a significant decrease

in the size of the low-electron-density regions, while these regions are slightly enlarged in the case of silicon adsorption in the Top(Ta) and Q positions.

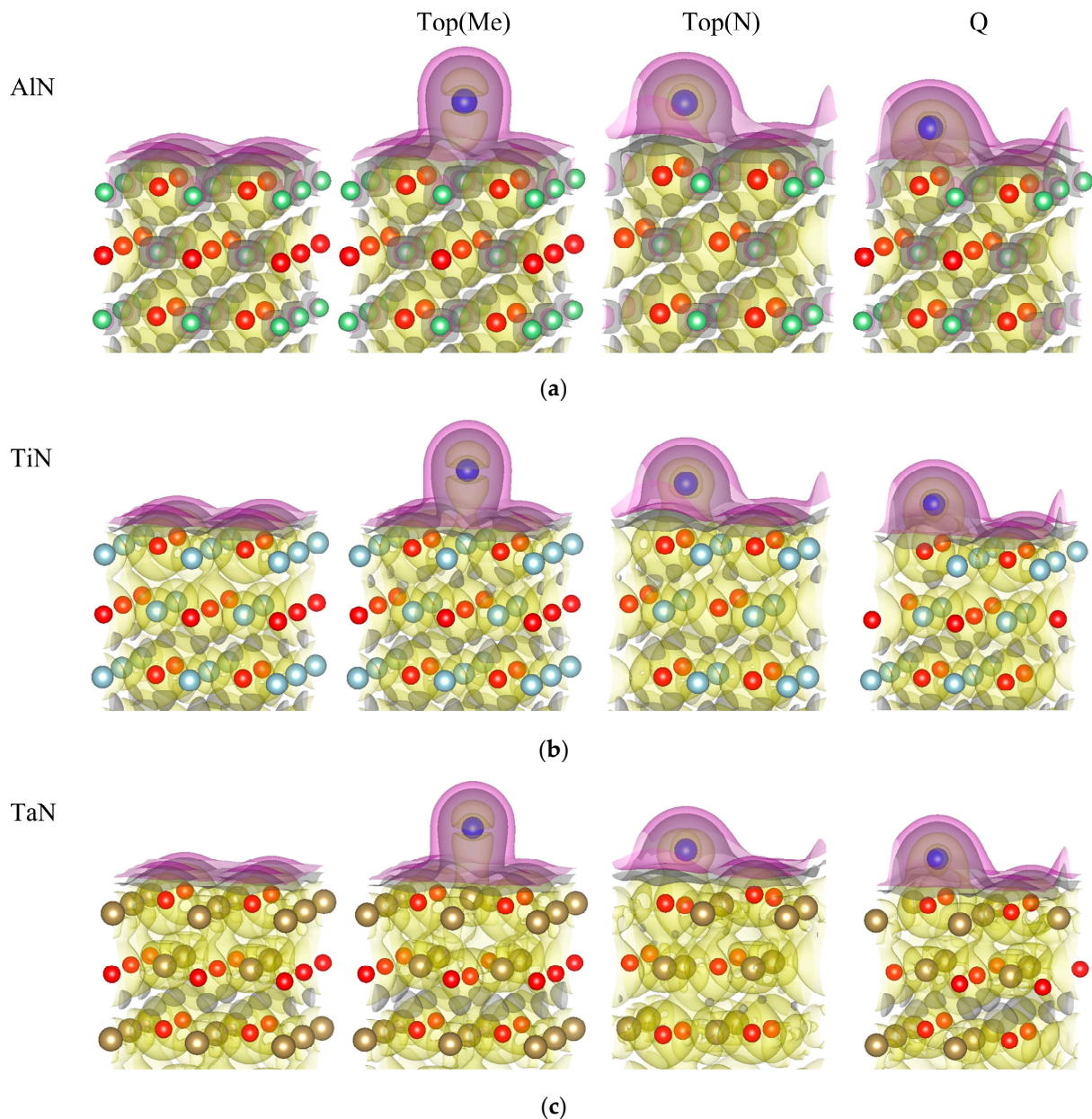


Figure 4. Valence electron density distribution on the (001) surface of the (a) AlN, (b) TiN and (c) TaN films without and with the Si atom. The yellow, gray, and pink isosurfaces correspond to charge densities of 0.05, 0.02, and 0.01 electron/Å³, respectively. The black, green, and purple balls are titanium, aluminum, and tantalum atoms, respectively. The red balls are nitrogen atoms; the blue balls are silicon atoms.

For the detailed analysis of the valence electron density distribution, the Bader charge transfer on the (001) surface of AlN, TiN, and TaN compounds was calculated. The results of the calculation are presented in Tables 2 and 3. Figure 5 shows the change in the Bader charge transfer on the (001) surface of AlN, TiN, and TaN compounds due to the silicon adsorption.

$$\Delta Q = Q_{\text{Si}} - Q_{\text{clean}} \quad (4)$$

where Q_{Si} and Q_{clean} are the Bader charge transfers in the atom of the considered system in the presence and absence of the silicon atom adsorbed on the surface, respectively.

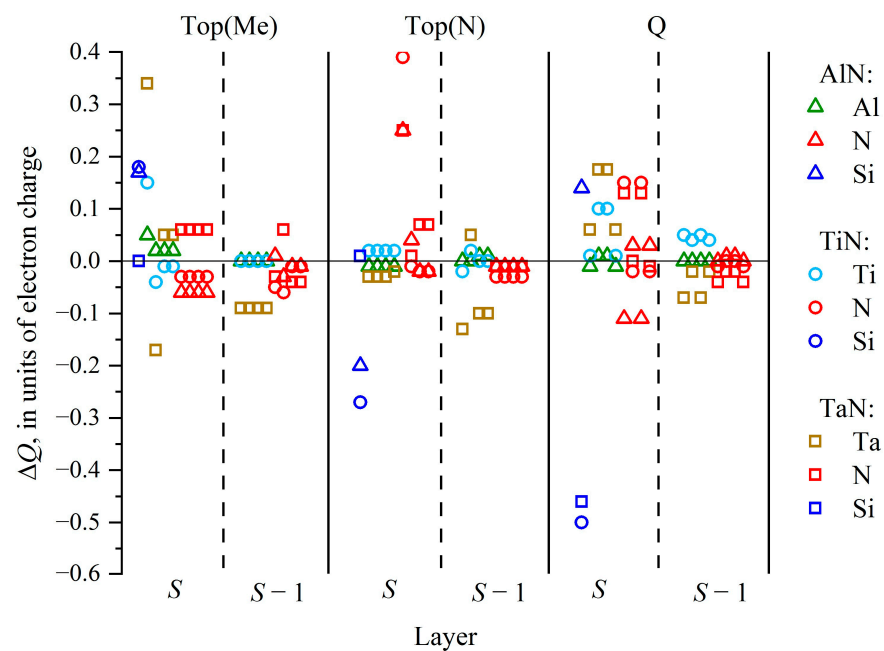


Figure 5. The change in the Bader charge transfer in the atoms of the surface (S) and subsurface (S − 1) atomic layers of AlN, TiN, and TaN films due to the silicon adsorption in different positions.

Table 2. The Bader charge transfer (in units of electron charge) in the atoms of the surface (S) and subsurface (S − 1), (S − 2) atomic layers of the AlN film due to the silicon adsorption in the different positions.

Layer	Atom	Clean	Top(Al)	Top(N)	Q
S	Si	-	0.17	−0.20	0.14
	Al1	−2.30	−2.25	−2.31	−2.31
	Al2	−2.30	−2.29	−2.31	−2.29
	Al3	−2.30	−2.29	−2.31	−2.29
	Al4	−2.30	−2.29	−2.31	−2.31
	N1	2.30	2.24	2.55	2.18
	N2	2.30	2.24	2.30	2.33
	N3	2.30	2.24	2.29	2.18
	N4	2.30	2.24	2.29	2.33
S − 1	Al5	−2.33	−2.33	−2.33	−2.33
	Al6	−2.33	−2.33	−2.33	−2.33
	Al7	−2.33	−2.33	−2.32	−2.33
	Al8	−2.33	−2.33	−2.32	−2.33
	N5	2.35	2.35	2.34	2.34
	N6	2.35	2.32	2.34	2.35
	N7	2.35	2.34	2.34	2.35
	N8	2.35	2.34	2.34	2.34
S − 2	Al9	−2.34	−2.32	−2.33	−2.33
	Al10	−2.34	−2.34	−2.33	−2.34
	Al11	−2.34	−2.33	−2.33	−2.34
	Al12	−2.34	−2.33	−2.33	−2.33
	N9	2.33	2.32	2.32	2.34
	N10	2.33	2.32	2.33	2.33
	N11	2.33	2.32	2.34	2.34
	N12	2.33	2.32	2.34	2.33

Table 3. The Bader charge transfer (in units of electron charge) in the atoms of the surface (S) and subsurface ($S - 1$), ($S - 2$) atomic layers of the TiN and TaN films due to the silicon adsorption in the different positions.

Layer	TiN(001)					TaN(001)				
	Atom	Clean	Top(Ti)	Top(N)	Q	Atom	Clean	Top(Ta)	Top(N)	Q
S	Si	-	0.18	-0.27	-0.50	Si	-	0.00	0.01	-0.46
	Ti1	-1.51	-1.36	-1.49	-1.50	Ta1	-1.58	-1.24	-1.61	-1.52
	Ti2	-1.51	-1.55	-1.49	-1.41	Ta2	-1.58	-1.75	-1.61	-1.39
	Ti3	-1.51	-1.51	-1.49	-1.41	Ta3	-1.58	-1.53	-1.61	-1.42
	Ti4	-1.51	-1.51	-1.49	-1.50	Ta4	-1.59	-1.53	-1.61	-1.53
	N1	1.47	1.44	1.85	1.62	N1	1.51	1.57	1.75	1.63
	N2	1.47	1.44	1.46	1.45	N2	1.51	1.57	1.51	1.51
	N3	1.47	1.44	1.44	1.62	N3	1.51	1.57	1.58	1.63
$S - 1$	N4	1.47	1.44	1.44	1.45	N4	1.51	1.57	1.58	1.50
	Ti5	-1.47	-1.47	-1.49	-1.42	Ta5	-1.52	-1.62	-1.65	-1.59
	Ti6	-1.47	-1.47	-1.45	-1.43	Ta6	-1.52	-1.62	-1.48	-1.54
	Ti7	-1.47	-1.47	-1.47	-1.42	Ta7	-1.52	-1.62	-1.62	-1.60
	Ti8	-1.47	-1.47	-1.47	-1.43	Ta8	-1.52	-1.62	-1.62	-1.54
	N5	1.52	1.47	1.49	1.50	N5	1.59	1.56	1.58	1.55
	N6	1.52	1.46	1.49	1.51	N6	1.59	1.65	1.58	1.57
	N7	1.52	1.50	1.49	1.51	N7	1.59	1.55	1.58	1.57
$S - 2$	N8	1.52	1.50	1.49	1.50	N8	1.59	1.55	1.58	1.55
	Ti9	-1.50	-1.50	-1.50	-1.50	Ta9	-1.66	-1.71	-1.64	-1.63
	Ti10	-1.50	-1.51	-1.50	-1.51	Ta10	-1.66	-1.70	-1.64	-1.65
	Ti11	-1.50	-1.49	-1.50	-1.51	Ta11	-1.66	-1.68	-1.64	-1.63
	Ti12	-1.50	-1.49	-1.50	-1.50	Ta12	-1.66	-1.68	-1.64	-1.65
	N9	1.51	1.51	1.51	1.48	N9	1.61	1.65	1.65	1.58
	N10	1.51	1.51	1.50	1.50	N10	1.61	1.65	1.67	1.58
	N11	1.51	1.51	1.51	1.48	N11	1.61	1.65	1.57	1.58
$S - 2$	N12	1.51	1.51	1.51	1.50	N12	1.61	1.65	1.57	1.58

In the bulk AlN crystal, the Bader charge transfer from the Al to N atom is equal to 2.29 electrons. In the surface and subsurface atomic layers of the clean AlN(001) film, the Bader charge transfer from the Al to N atom varies insignificantly (from 2.30 to 2.35 electrons) and is close to the bulk value (see Table 2). This confirms the previously mentioned conclusion about the purely ionic type of bonding between the atoms of the AlN compound. Silicon adsorption leads to a noticeable redistribution of an electron charge only in the surface layer; in the subsurface ($S - 1$) and ($S - 2$) layers, the change in the Bader charge transfer due to silicon adsorption does not exceed 0.03 electrons (see Figure 5). The Bader charge transfer (~ 0.2 electron) to silicon adsorbed in the Top(Al) position occurs from the N atoms surrounding the Al atom nearest to the Si atom and from silicon in the Top(N) position to the nearest nitrogen atom. When the Si atom is adsorbed in the Q position, the Bader charge transfer of 0.14 electrons to silicon is observed from the nearest nitrogen atoms. In all of the silicon positions considered, except for the Top(Al) position, the change in charge of the aluminum atoms is insignificant. When the Si atom adsorbs in the Top(Al) position, the nearest Al atom takes 0.05 electrons. Thus, adsorption of silicon on the AlN(001) surface causes the valence electron density redistribution between silicon and surface nitrogen atoms predominantly.

In the bulk of TiN and TaN, the Bader charge transfer from the metal atoms to the nitrogen atoms is equal to 1.46 and 1.55 electrons, respectively, which is less than in the bulk of AlN. The close values of the charge transfer in TiN and TaN, despite the different number of valence electrons in the Ti and Ta atoms (four and five electrons, respectively), indicate that the nitrogen atoms in these compounds take on a predominantly electronic charge from the metal s states. In the surface and subsurface atomic layers of the clean TiN(001) film, the Bader charge transfer from the Ti atom to the N atom varies insignificantly (from

1.47 to 1.52 electrons) and is close to the bulk value (see Table 3). In the clean TaN(001) film, the charge transfer varies much more in the surface layers than in the TiN(001) film, from 1.51 to 1.66 electrons, and even differs significantly from the bulk value in the subsurface ($S - 2$) layers. This may be caused by a high degree of corrugation in the surface and subsurface atomic layers of the TaN film.

Silicon adsorption on the TiN(001) surface leads to a noticeable redistribution of the electron charge only in the surface layer, as on the AlN(001) surface. In the case of the TaN(001) film, the adsorbed Si atom causes a significant redistribution of the electron charge in the surface and subsurface ($S - 1$) layers. In the subsurface ($S - 2$) layer of the TiN and TaN films, the change in the Bader charge transfer due to silicon adsorption does not exceed 0.01 and 0.05 electrons, respectively (see Figure 5). As on the AlN(001) surface, the Si atom adsorbed on the TiN(001) surface takes 0.18 electrons from the surface and subsurface nitrogen atoms in the Top(Ti) position and gives 0.27 electrons to the nearest nitrogen atom in the Top(N) position. On the TaN(001) surface, the Si atom is neutral in the Top(Ta) and Top(N) positions: the Bader charge transfer for it is zero. The largest Bader charge transfer in the Si atom is observed when it is adsorbed in the Q position on the TiN and TaN surfaces; in these cases, 0.50 and 0.46 electrons, respectively, are transferred from the silicon to the metal atoms and nitrogen. This indicates a high degree of ionic bonding of silicon at the Q position with the (001) surface of TiN and TaN compounds.

3.4. Density of States and Bond Strength

Figure 6 shows the calculated total density of states of the bulk AlN, TiN, and TaN crystals and their clear films (001) and films with silicon adsorbed in three symmetrical positions. As can be seen in Figure 6, the bulk AlN compound is an insulator with a band gap of ~4.3 eV, and the TiN and TaN compounds are metals with a sufficiently high density of electronic states at the Fermi level. The calculated total densities of states of bulk TiN and TaN are in good agreement with the results of the DFT calculations [32,45]. Unfortunately, we could not find any information on the electronic structure of the AlN compound in the high-temperature phase with the NaCl structure.

The total density of states of the clean AlN(001) film has almost the same form as the DOS of the bulk compound except for two peculiarities: the appearance of a peak in the energy region around -1.1 eV and the structure consisting of two peaks in the energy range from 2.5 to 5.0 eV. The band gap of ~2.5 eV of the AlN(001) film is less than the bulk band gap. These features seem to be related to the appearance of surface electron states near these energies on the surface of this film. Unfortunately, we were unable to find any information on the electronic structure of the surface (001) of the AlN compound in the NaCl structure.

The total density of states of the clean TiN(001) and TaN(001) films are also virtually indistinguishable in shape from the DOS of the bulk compounds, except for some features most likely related to the appearance of surface states. For TiN, this is manifested by a broadening of the film DOS peak around -5.0 eV and an increase in the DOS peak height around 2.3 eV. For the TaN(001) film, the modification of the rather sharp bulk DOS peak around -6.9 eV into two overlapping peaks in the range of -6.8 to -5.3 eV is observed. Furthermore, in the TaN(001) film, the DOS peak appears in the region of the Fermi level, indicating a possible reconstruction of this surface structure.

Silicon deposition significantly modifies the DOS of the AlN(001) film, which can be seen in the metallization of the film spectrum due to the appearance of electronic states in the region of the Fermi level, indicating a possible reconstruction of this surface structure. It should be noted that in the case of silicon adsorption in the Q position, the density of electron states at the Fermi level is extremely low, indicating the stability of this surface structure. We add that the adsorption of silicon in exactly this position is characterized by the maximum binding energy of the adsorbate on this surface. This may indicate that in the case of epitaxial deposition of silicon on the AlN(001) surface, the adsorbate will occupy the Q position.

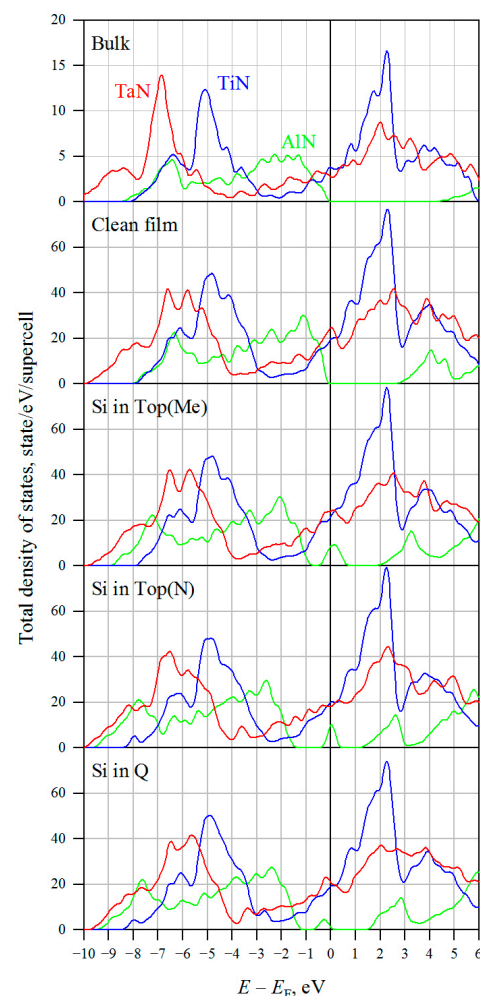


Figure 6. Total density of states of bulk AlN, TiN, and TaN crystals (top panel), clean films (001) (second-top panel) and films with silicon adsorbed in three symmetrical positions: Top(Me), Top(N), and Q.

The deposition of silicon on the TiN(001) surface does not result in a significant modification of the DOS film. The same can be observed for the adsorption of silicon in the Top(Me) and Q positions on the TaN(001) surface. However, it should be pointed out that the adsorption of silicon in these positions does not lead to the disappearance of the DOC peak at the Fermi level and thus does not eliminate the cause of the possible reconstruction of these surface structures. In the case of silicon adsorption in the Top(N) position on the TaN(001) surface, the DOS peak observed on a clean surface disappears, indicating that silicon stabilizes this surface. We add that the adsorption of silicon in the Top(N) position on the TaN(001) surface is characterized by the highest adsorbate binding energy on this surface. Based on this fact, we can assume that during the epitaxial deposition of silicon on the TaN(001) surface, the adsorbate will occupy the Top(N) position.

Figure 7 shows the local partial densities of states of the bulk atoms and surface layer atoms of the (001) films. The lower panel shows the -pCOHP for pairs of atoms in the bulk (Al_b-N_b), on the surface (Al_s-N_s) and for atoms in the surface and subsurface layers (N_s-Al_{s-1} , Al_s-N_{s-1}). We see that in the AlN compound, almost all the valence orbitals of aluminum and nitrogen make a positive contribution to the bonding forces between the atoms. The small negative contribution to the bonding is observed in the region from -1.1 eV up to the Fermi level, caused by interaction between the p orbitals of the Al_s and N_{s-1} atoms. In the compounds of nitrogen with the transition metals Ti and Ta, the picture is more complicated. In the compound TiN, the positive contribution to the bonding is

given by orbitals lying in the range of -8.0 to -2.4 eV. From -2.4 eV up to the Fermi level, there are orbitals that do not participate in the bonding. All orbitals above the Fermi level are unoccupied, otherwise they would weaken the interatomic bonds in TiN. In the TaN compound, the positive contribution to bonding is given by orbitals lying in the -9.7 to -3.8 eV region. In the region from -3.8 to -3.0 eV, there are the nonbonding orbitals, and from -3.0 to 0.5 eV, there are the orbitals that give a weak loosening of the interatomic bonds.

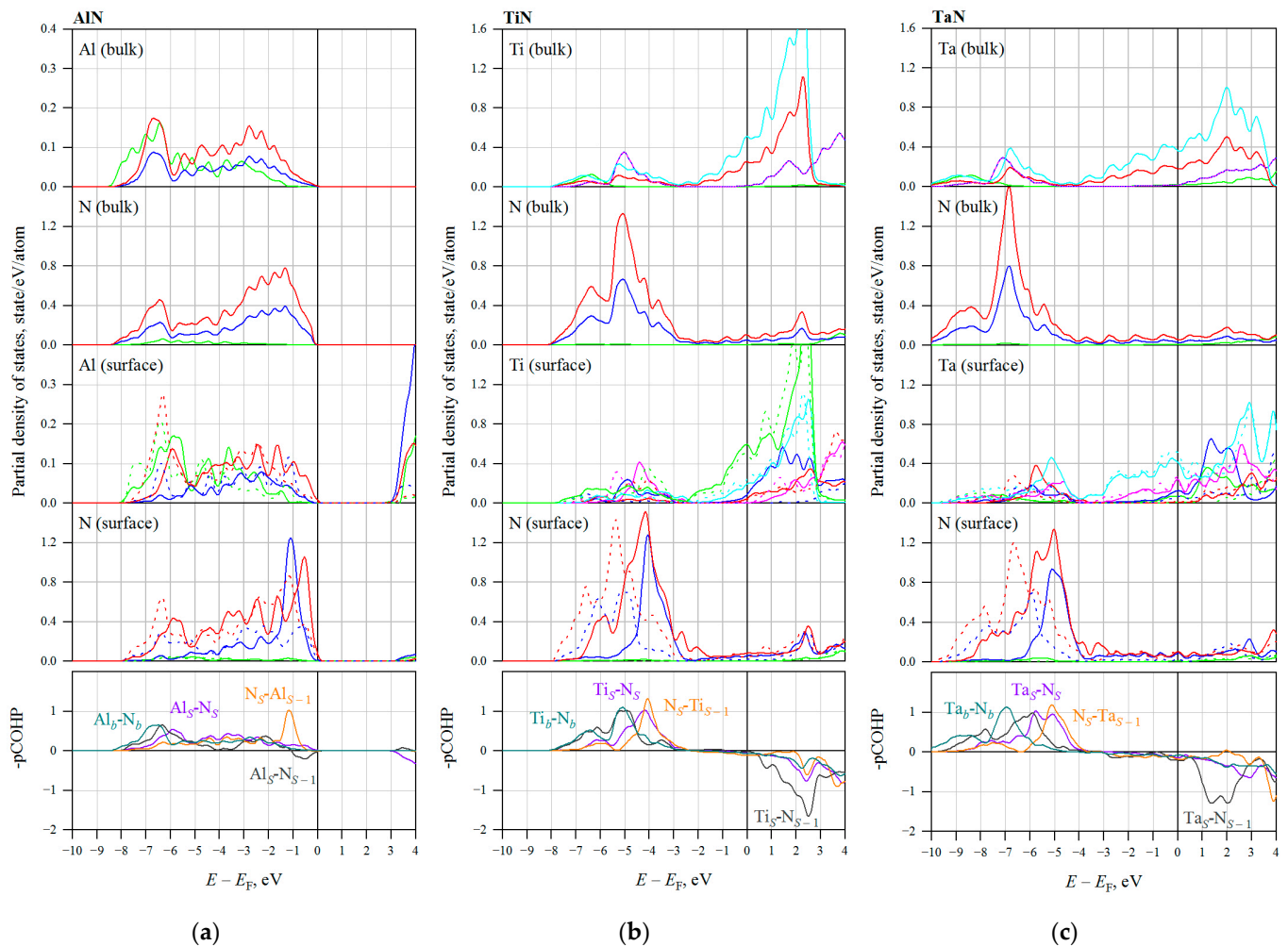


Figure 7. Partial density of states of the bulk and surface atoms and $-p\text{COHP}$ for pairs of atoms in the bulk, on the surface, and for atoms on the surface and in the subsurface layer of (a) AlN(001), (b) TiN(001), and (c) TaN(001) films. The densities of the s states are shown in green; the sum of the densities of the p_x and p_y states of N and Al or the densities of the d_{xy} states of Ti and Ta are shown in red; the densities of the p_z states of N and Al or the d_{zz} states of Ti and Ta are shown in blue; the densities of the $d_{x^2-y^2}$ states and the sum of the densities of the d_{xz} and d_{yz} states of Ti and Ta are shown in pink and blue, respectively. The solid and dashed lines correspond to the atoms of the surface and subsurface layers, respectively. The indices S , $S-1$, and b in the $-p\text{COHP}$ designations for the considered bonds denote the atoms of the surface, subsurface, and bulk layers, respectively.

Figure 8 shows the local partial densities of the states of the silicon atom adsorbed in the Top(Me) position and the surface layer atoms of the (001) films. The bottom two panels show $-p\text{COHP}$ for the silicon atom and surface layer atoms (Si-Me_S , Si-N_S), and surface and subsurface layer atoms ($\text{Me}_S\text{-N}_S$, $\text{Me}_S\text{-N}_{S-1}$). It can be seen that when silicon is adsorbed in the Top(Me) position on the AlN(001) surface, its s orbitals hybridize with the s and p_z orbitals of Al to form binding states in the energy range from -8.7 to -5.9 eV. Bonding states are also observed in the energy range -0.5 to 0.6 eV, but now they are formed by

p_x - p_y and p_z orbitals of silicon and s - p_z orbitals of Al. In the energy range of -0.5 to 0.6 eV, the antibonding states are formed between Si-N_S and $\text{Al}_S\text{-N}_S$ atom pairs. The character of bonding between the $\text{Al}_S\text{-N}_S$ and $\text{Al}_S\text{-N}_{S-1}$ atom pairs in the range of -8.7 to -1.0 eV is the same as on the clean surface in the range of -8.0 to the Fermi level. In compounds of nitrogen with the transition metals Ti and Ta, bonding between the silicon and metal atoms is mainly observed. The formation of binding states upon hybridization of Si p_z orbitals with Ti d_{z2} orbitals at -0.4 eV leads to the appearance of antibonding states between surface Ti_S and subsurface N_{S-1} atom. The adsorption of silicon in the Top(Ti) position slightly changes the nature of the interaction between $\text{Ti}_S\text{-N}_S$ atoms, but markedly weakens the bond between $\text{Ti}_S\text{-N}_{S-1}$ atoms in the energy range from -8.0 to -2.4 eV. A similar pattern is observed for the adsorption of silicon on the TaN surface, but the weakening of the $\text{Ta}_S\text{-N}_{S-1}$ bond is significantly stronger than that of the $\text{Ti}_S\text{-N}_{S-1}$ bond on the TiN surface.

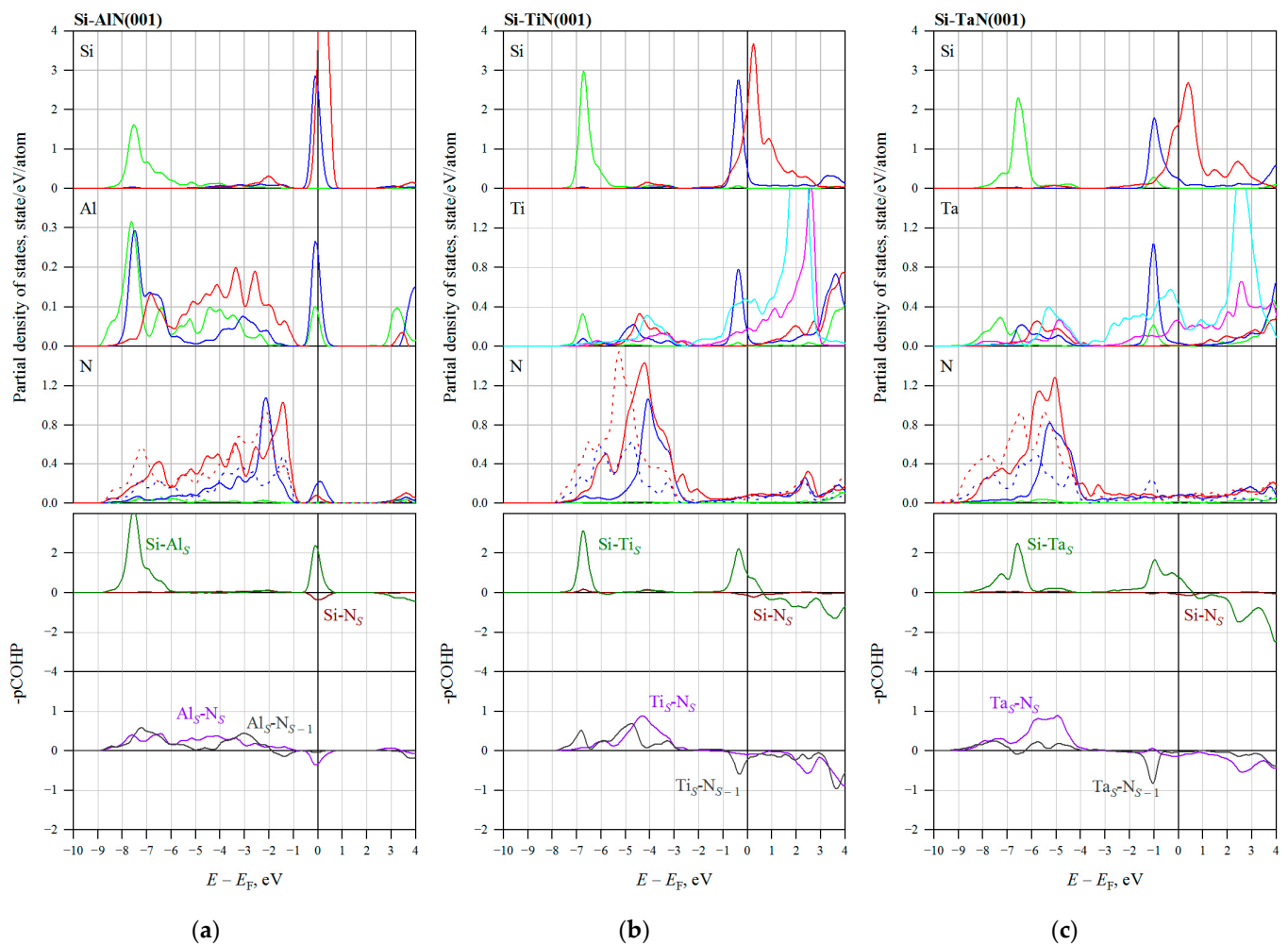


Figure 8. Partial density of states of the Si atom in the Top(Me) position and surface atoms and -pCOHP for pairs of atoms on the surface and in the subsurface layer of (a) AlN(001), (b) TiN(001), and (c) TaN(001) films. The densities of the s states are shown in green; the sum of the densities of the p_x and p_y states of Si, N, and Al or the densities of the d_{xy} states of Ti and Ta are shown in red; the densities of the p_z states of Si, N, and Al or the d_{z2} states of Ti and Ta are shown in blue; the densities of the d_{x2-y2} states and the sum of the densities of the d_{xz} and d_{yz} states of Ti and Ta are shown in pink and blue, respectively. The solid and dashed lines correspond to the atoms of the surface and subsurface layers, respectively. The indices S , $S-1$, and b in the -pCOHP designations for the considered bonds denote the atoms of the surface, subsurface, and bulk layers, respectively.

Figure 9 shows the local partial densities of the states of the silicon atom adsorbed in the position above nitrogen and the surface layer atoms of the (001) films. The bottom

two panels show the -pCOHP for the silicon atom and the surface layer atoms (Si-Me_S, Si-N_S) and the surface and subsurface layer atoms (N_S-Me_S, N_S-Me_{S-1}). It can be seen that when silicon is adsorbed in this position on the AlN(001) surface, its orbitals hybridize with the N *p_z* orbital to form the bonding states in the energy range from -9.6 to -7.9 eV. Bonding is also observed in the -7.9 to -2.9 eV energy range, but is weaker and is formed by the *s* orbital of Si and the *p_x*-*p_y* orbitals of nitrogen. Near the Fermi level (-0.5 to 0.5 eV), the hybridization of the *s* orbitals of silicon and nitrogen is observed, giving rise to the antibonding interaction that weakens the Si-N bond. In the same energy range is the -pCOHP peak, formed by the binding hybridization of the *p_x*-*p_y* orbitals of silicon with the *p_z* orbital of Al. On the TiN(001) surface, in the energy range from -8.4 to -7.5 eV, there is a higher binding peak of -pCOHP due to hybridization of the *s* orbital of Si with the *p_z* orbital of N, forming the bonding states. In the region of energies above -4.0 eV the hybridization of the same states already gives an antibonding contribution to the binding energy. The adsorption of Si on the TaN(001) surface does not give as high a binding peak of the -pCOHP as on the TiN(001) surface, but the range of binding interactions extends from -10.0 to -7.1 eV. The adsorption of silicon over the nitrogen on the surface of all considered compounds strongly changes the nature of bonding of this N atom with the surface (Al_S, Ti_S and Ta_S) and subsurface (Al_{S-1}, Ti_{S-1} and Ta_{S-1}) nearest neighbors. The hybridization of Si *s* orbitals with N *s*-*p_z* orbitals leads to the appearance of binding states between all considered atom pairs in the energy range from -9.5 to 6.8 eV, from -8.5 to -7.6 eV, and from -10.0 to -7.1 eV on the surface of AlN, TaN, and TaN, respectively.

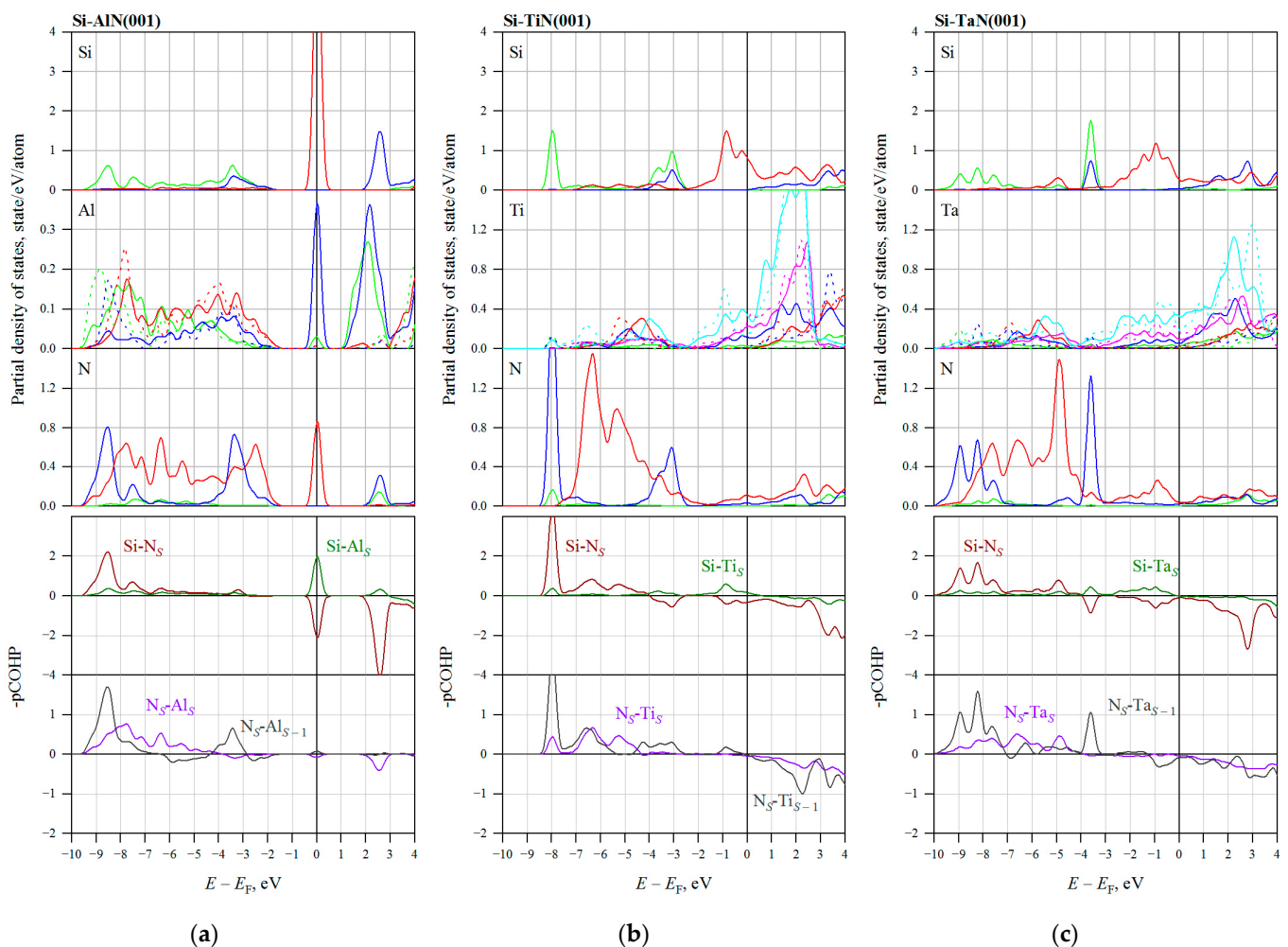


Figure 9. Partial density of states of the Si atom in the Top(N) position and surface atoms and -pCOHP for pairs of atoms on the surface and in the subsurface layer of (a) AlN(001), (b) TiN(001),

and (c) TaN(001) films. The densities of the s states are shown in green; the sum of the densities of the p_x and p_y states of Si, N and Al or the densities of the d_{xy} states of Ti and Ta are shown in red; the densities of the p_z states of Si, N and Al or the d_{z^2} states of Ti and Ta are shown in blue; the densities of the $d_{x^2-y^2}$ states and the sum of the densities of the d_{xz} and d_{yz} states of Ti and Ta are shown in pink and blue, respectively. The solid and dashed lines correspond to the atoms of the surface and subsurface layers, respectively. The indices S , $S-1$, and b in the -pCOHP designations for the considered bonds denote the atoms of the surface, subsurface, and bulk layers, respectively.

Figure 10 shows the local partial state densities of the silicon atom adsorbed in the Q position and the surface layer atoms of the (001) films. The bottom two panels show the -pCOHP for the silicon atom and the surface layer atoms (Si-Me_S, Si-N_S) and the surface and subsurface layer atoms (N_S-Me_S, Me_S-N_{S-1} and N_S-Me_{S-1}). It can be seen that the adsorption of silicon in this position on the AlN(001) surface in the energy range from -9.5 to -1.4 eV shows a rather flat and not high plateau of Si-N and Si-Al binding interactions. At higher energies, there is the high peak of the Si-Al bonding state in the occupied part of the spectra, while the Si-N interaction gives the small antibonding peak in this energy region. The TiN(001) and TaN(001) surfaces show a slightly different pattern. There is the characteristic low energy binding peak of the Si-N interaction (in the region of -8.0 and -8.8 eV for TiN and TaN, respectively) and the rather broad plateau of the Si-Me bonding interaction in the region from -2.0 eV to the Fermi level. The Si-Me interaction becomes antibonding at energies above -2.9 eV / -3.7 eV on the (001) surface of the TiN/TaN compounds. In the vicinity of the Fermi energy, all the hybridized Si-Me states are bonding and all the hybridized Si-N states are antibonding, which is also observed for the other silicon adsorption positions considered (see Figures 8 and 9). Adsorption of silicon in the Q position weakly affects the bond between Me_S and N_{S-1} atoms, significantly weakens the bond between the nearest surface metal and nitrogen atoms, and strongly changes the shape of the -pCOHP curves for the N_S and Me_{S-1} atom pair.

In order to analyze in detail the bond strength of Si-N and Si-Me on the considered surface, as well as to reveal the influence of silicon adsorption on the bonding between surface Me and N atoms, the -pCOHP curves were integrated over the energy from -10 eV up to the Fermi level. Integrating the -pCOHP values over the energy up to the Fermi level (-IpCOHP) for a pair of atoms gives the bond strength in terms of its contribution to the band structure energy [46–48]. The results of the calculations are presented in Table 4. The strongest Si-Me_S bonds are observed in the adsorption of silicon in the Top(Me) position. The strongest bond is formed between Al and Si atoms. At the same time, the bonding of silicon to more distant nitrogen atoms is weak: the -IpCOHP values for Si-N_S bonds range from 0.124 to 0.160. When silicon is adsorbed in the Top(N) position, strong silicon bonds are observed with both the nearest nitrogen atom (-IpCOHP values for Si-N_S bonds range from 2.007 to 2.460) and the four more distant metal atoms on the surface (-IpCOHP values for Si-Me_S bonds range from 1.015 to 1.513). This explains the higher bond energies of silicon in the Top(N) position. The high Si-Me_S and Si-N_S bond strengths are also observed when silicon is adsorbed in the Q position, but silicon accepts 0.50 and 0.46 electrons (Figure 5) on the Ti-N and Ta-N surfaces, respectively, which leads to its repulsion from the nearest negatively charged nitrogen atoms and lowers the bond energies of Si-Me_S and Si-N_S. When silicon is adsorbed on the AlN surface, an electron charge transfer of $0.14 e$ is observed from the silicon atom (Figure 5), which favors its additional attraction to the nearest negatively charged nitrogen atoms. As a result of this additional attraction, we observe a higher binding energy of silicon in the Q position compared to the Top(N) position (Figure 3).

The analysis of the -IpCOHP values presented in Table 4 for the N_S-Me_S bonds showed that the adsorption of silicon in any position on the (001) surface of the considered compounds significantly weakens the N_S-Me_S bonds. The change in the bond strength between surface and subsurface atoms depends on the position of the silicon atom and the considered compound. Thus, when silicon is adsorbed in the Top(Me) position, the

strength of the $\text{Me}_S\text{-N}_{S-1}$ bond on the surface of the AlN compound increases slightly and decreases significantly on the surface of the TiN and TaN compounds (the $-\text{IpCOHP}$ value for $\text{Ti}_S\text{-N}_{S-1}$ and $\text{Ta}_S\text{-N}_{S-1}$ bonds decreases by ~ 1). For the adsorption of silicon in the Top(N) position, a qualitatively opposite picture is observed: the strength of the $\text{N}_S\text{-Me}_{S-1}$ bond decreases on the surface of the AlN compound and slightly increases on the surface of the TiN and TaN compounds. As mentioned above, silicon adsorption in the Q position weakly affects the bond between Me_S and N_{S-1} atoms and strongly modifies the $\text{N}_S\text{-Me}_{S-1}$ bonds, reducing their strength. It should be noted that silicon adsorption in this position slightly strengthens the bonds between $\text{Al}_S\text{-N}_{S-1}$ and $\text{Ta}_S\text{-N}_{S-1}$, and weakens the bond between $\text{Ti}_S\text{-N}_{S-1}$.

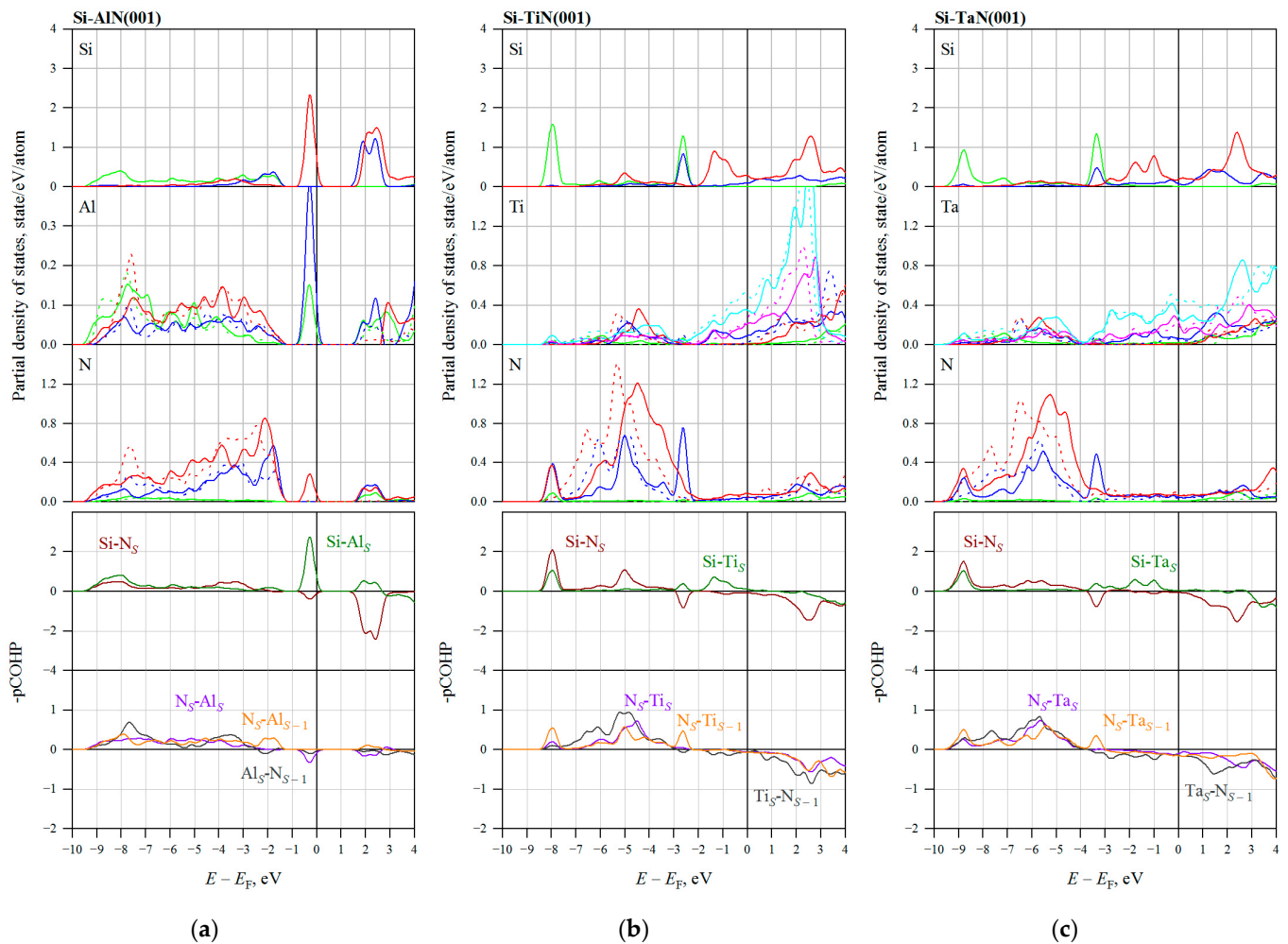


Figure 10. Partial density of states of the Si atom in the Q position and surface atoms and $-\text{pCOHP}$ for pairs of atoms on the surface and in the subsurface layer of (a) AlN(001), (b) TiN(001), and (c) TaN(001) films. The densities of the s states are shown in green; the sum of the densities of the p_x and p_y states of Si, N, and Al or the densities of the d_{xy} states of Ti and Ta are shown in red; the densities of the p_z states of Si, N and Al or the d_{z2} states of Ti and Ta are shown in blue; the densities of the d_{x2-y2} states and the sum of the densities of the d_{xz} and d_{yz} states of Ti and Ta are shown in pink and blue, respectively. The solid and dashed lines correspond to the atoms of the surface and subsurface layers, respectively. The indices S , $S-1$, and b in the $-\text{pCOHP}$ designations for the considered bonds denote the atoms of the surface, subsurface, and bulk layers, respectively.

Table 4. The results of integrating the -pCOHP values (-IpCOHP) over the energy from −10 eV up to the Fermi level for all the bonds considered.

System	Si-N _S Bond	Si-Me _S Bond	N _S -Me _S Bond	Me _S -N _{S-1} Bond	N _S -Me _{S-1} Bond	Me _b -N _b Bond
AlN	-	-	1.949	1.426	1.788	
AlN-Si ^{Top(Me)}	0.160	4.224	1.689	1.491	-	1.932
AlN-Si ^{Top(N)}	2.432	1.306	1.614	-	1.656	
AlN-Si ^Q	1.777	3.358	1.240	1.567	1.657	
TiN	-	-	1.701	2.062	1.318	
TiN-Si ^{Top(Me)}	0.191	2.901	1.490	1.091	-	1.918
TiN-Si ^{Top(N)}	2.460	1.015	1.178	-	2.223	
TiN-Si ^Q	1.914	1.636	1.210	1.831	1.259	
TaN	-	-	1.938	1.295	1.953	
TaN-Si ^{Top(Me)}	0.124	4.046	1.848	0.179	-	1.880
TaN-Si ^{Top(N)}	2.007	1.513	1.299	-	2.230	
TaN-Si ^Q	1.905	1.949	1.347	1.515	1.343	

4. Conclusions

In the present paper, the ab initio study of the features of the interaction of a silicon atom with the (001) surface of AlN, TiN, and TaN compounds was performed within the framework of the density functional theory. The main conclusions were drawn as follows.

1. It was shown that on the clean (001) surface of TiN and TaN, significant relaxation and corrugation of the surface layers are observed. Silicon adsorption on the (001) surface of AlN, TiN, and TaN compounds leads to an increase in both the relaxation and corrugation. The largest corrugation is observed on the surface of the TaN compound. The smallest influence of silicon adsorption on the surface relaxation is observed on the surface of the AlN compound. It is found that the surface relaxation is slightly dependent on the silicon-adsorption position.

2. The adsorption of silicon on the (001) surface of the AlN, TiN, and TaN compounds is characterized by a positive binding energy (from 1.0 to 5.4 eV). The position of Si above the N atom is most energetically favorable on the TiN(001) and TaN(001) surfaces. In the case of the AlN(001) surface, the quadruple coordinated position is most energetically favorable for silicon adsorption. The bridge positions of Si are unstable for all surfaces considered. On the TaN surface, silicon is found to have the highest binding energy, while on the AlN surface, it has the lowest.

3. When adsorbed on the (001) surface, silicon forms predominantly covalent bonds with the nearest metal and nitrogen atoms, except for the quadruple coordinated position on the TiN and TaN surface, where there is a high degree of ionic bonding of silicon with surface atoms. On the TaN(001) surface, the Si atom is neutral in the positions above the Ta and N atoms.

4. The Si atom adsorbed on the surface of AlN, TiN, and TaN forms the bonding states with the nearest surface atoms in the regions from −9 to −3 eV, from −8.5 to −4 eV and from −10 to −4 eV below the Fermi energy, respectively. Near the Fermi energy, all the hybridized Si-Me states are bonding and all the hybridized Si-N states are antibonding. The strongest bonds are observed between the silicon in the top position and the metal atom below. Silicon adsorption on the (001) surface of the AlN, TiN, and Ta compounds significantly weakens the bonds between the nearest surface nitrogen and metal atoms. The change in bond strength between surface and subsurface nitrogen and metal atoms with silicon adsorption depends on its position and the compound.

The information about the nature of silicon bonding with metal and nitrogen atoms on the of AlN(001), TiN(001), and TaN(001) surfaces obtained in this work will be used in the future to model the processes of sorption of silicon on the surface of a multicomponent Ti-Al-Ta-Si-N film and the formation of different crystalline phases using molecular dynamics methods.

Author Contributions: Conceptualization, L.S. and Y.K.; methodology, S.O. and Y.K.; formal analysis, L.S., S.O., M.S. and Y.K.; investigation, L.S. and S.O.; writing—original draft preparation, L.S., S.O., M.S. and Y.K.; visualization, L.S. and S.O.; supervision, Y.K. All authors have read and agreed to the published version of the manuscript.

Funding: This work was funded by the Russian Science Foundation, research project No. 22-19-00441.

Institutional Review Board Statement: Not applicable.

Informed Consent Statement: Not applicable.

Data Availability Statement: The data presented in this study are available on request from the corresponding author. The data are not publicly available due to privacy reasons.

Conflicts of Interest: The authors declare no conflict of interest.

References

1. PalDey, S.; Deevi, S.C. Single layer and multilayer wear resistant coatings of (Ti, Al)N: A review. *Mater. Sci. Eng. A* **2003**, *342*, 58–79. [\[CrossRef\]](#)
2. Bartosik, M.; Rumeau, C.; Hahn, R.; Zhang, Z.L.; Mayrhofer, P.H. Fracture toughness and structural evolution in the TiAlN system upon annealing. *Sci. Rep.* **2017**, *7*, 16476. [\[CrossRef\]](#) [\[PubMed\]](#)
3. Shugurov, A.R.; Kuzminov, E.D.; Kasterov, A.M.; Panin, A.V.; Dmitriev, A.I. Tuning of mechanical properties of Ti_{1-x}Al_xN coatings through Ta alloying. *Surf. Coat. Technol.* **2020**, *382*, 125219. [\[CrossRef\]](#)
4. Hollerweger, R.; Riedl, H.; Paulitsch, J.; Arndt, M.; Rachbauer, R.; Polcik, P.; Primig, S.; Mayrhofer, P.H. Origin of high temperature oxidation resistance of Ti–Al–Ta–N coatings. *Surf. Coat. Technol.* **2014**, *257*, 78–86. [\[CrossRef\]](#)
5. Miletic, A.; Panjan, P.; Skoric, B.; Cekada, M.; Drazic, G.; Kovac, J. Microstructure and mechanical properties of nanostructured Ti–Al–Si–N coatings deposited by magnetron sputtering. *Surf. Coat. Technol.* **2014**, *241*, 105–111. [\[CrossRef\]](#)
6. Pei, F.; Liu, H.J.; Chen, L.; Xu, Y.X.; Du, Y. Improved properties of TiAlN coating by combined Si-addition and multilayer architecture. *J. Alloys Compd.* **2019**, *790*, 909–916. [\[CrossRef\]](#)
7. Qin, H.; Tao, Y.; Deng, B. Microstructural and mechanical properties of Si-ion implanted TiN coatings. *Surf. Coat. Technol.* **2013**, *228*, S292–S295. [\[CrossRef\]](#)
8. Nah, J.W.; Choi, W.S.; Hwang, S.K.; Lee, C.M. Chemical state of (Ta, Si)N reactively sputtered coating on a high-speed steel substrate. *Surf. Coat. Technol.* **2000**, *123*, 1–7. [\[CrossRef\]](#)
9. Marques, L.; Carvalho, S.; Vaz, F.; Ramos, M.M.D.; Rebouta, L. ab-initio Study of the properties of Ti_{1-x-y}Si_xAl_yN solid solution. *Vacuum* **2009**, *83*, 1240–1243. [\[CrossRef\]](#)
10. Ereemeev, S.V.; Shugurov, A.R. Chemical bonding analysis in Ti_{1-x-y}Al_xTa_yN solid solutions. *Surf. Coat. Technol.* **2020**, *395*, 125802. [\[CrossRef\]](#)
11. Liu, X.; Lu, F.; Wu, S.; Ren, Y. Effects of different nitrogen-to-titanium atomic ratios on the evolution of Ti–Si–N islands on TiN(001) surfaces: First-principle studies. *J. Alloys Compd.* **2014**, *586*, 431–435. [\[CrossRef\]](#)
12. Ren, Y.; Zhang, H.; Zhang, C.; Zeng, H.; Liu, X. First-principles study of the charge transfer and evolution of Si doping 2N2Ta islands adsorption on TaN (001) surfaces. *Appl. Surf. Sci.* **2017**, *392*, 350–355. [\[CrossRef\]](#)
13. Gonze, X.; Amadon, B.; Antonius, G.; Arnardi, F.; Baguet, L.; Beuken, J.-M.; Bieder, J.; Bottin, F.; Bouchet, J.; Bousquet, E.; et al. The Abinit project: Impact, Environment and Recent Developments. *Comput. Phys. Commun.* **2020**, *248*, 107042. [\[CrossRef\]](#)
14. Romero, A.H.; Allan, D.C.; Amadon, B.; Antonius, G.; Applencourt, T.; Baguet, L.; Bieder, J.; Bottin, F.; Bouchet, J.; Bousquet, E.; et al. ABINIT: Overview and Focus on Selected Capabilities. *J. Chem. Phys.* **2020**, *152*, 124102. [\[CrossRef\]](#) [\[PubMed\]](#)
15. Blöchl, P.E. Projector augmented-wave method. *Phys. Rev. B* **1994**, *50*, 17953. [\[CrossRef\]](#)
16. Kresse, G.; Joubert, D. From ultrasoft pseudopotentials to the projector augmented-wave method. *Phys. Rev. B* **1999**, *59*, 1758. [\[CrossRef\]](#)
17. Perdew, J.P.; Burke, K.; Ernzerhof, M. Generalized Gradient Approximation Made Simple. *Phys. Rev. Lett.* **1996**, *77*, 3865–3868. [\[CrossRef\]](#)
18. Louhibi-Fasla, S.; Achour, H.; Kefif, K.; Ghalem, Y. First-principles study of high-pressure phases of AlN. *Phys. Proc.* **2014**, *55*, 324–328. [\[CrossRef\]](#)
19. Feldbauer, G.; Wolloch, M.; Bedolla, P.O.; Mohn, P.; Redinger, J.; Vernes, A. Adhesion and material transfer between contacting Al and TiN surfaces from first principles. *Phys. Rev. B* **2015**, *91*, 165413. [\[CrossRef\]](#)
20. Taehun Lee, T.; Delley, B.; Stampfl, C.; Soon, A. Environment-dependent nanomorphology of TiN: The influence of surface vacancies. *Nanoscale* **2012**, *4*, 5183–5188. [\[CrossRef\]](#)
21. Ren, Y.; Liu, X.; Tan, X.; Westkämper, E. Adsorption and pathways of single atomistic processes on TiN (111) surfaces: A first principle study. *Com. Mat. Sci.* **2013**, *77*, 102–107. [\[CrossRef\]](#)
22. Xia, Q.; Xia, H.; Ruoff, A.L. Pressure-induced rocksalt phase of aluminum nitride: A metastable structure at ambient condition. *J. Appl. Phys.* **1993**, *73*, 8198–8200. [\[CrossRef\]](#)

23. Zhang, R.; Ma, Q.-Y.; Liu, H.; Sun, T.-Y.; Bi, J.; Song, Y.; Peng, S.; Liang, L.; Gao, J.; Cao, H.; et al. Crystal Orientation-Dependent Oxidation of Epitaxial TiN Films with Tunable Plasmonics. *ACS Photonics* **2021**, *8*, 847–856. [\[CrossRef\]](#)
24. Phani, A.R.; Krzanowski, J.E. Preferential growth of Ti and TiN films on Si(111) deposited by pulsed laser deposition. *Appl. Surf. Sci.* **2001**, *174*, 132–137. [\[CrossRef\]](#)
25. Patel, N.; Wang, S.; Inspektor, A.; Salvador, P.A. Secondary hardness enhancement in large period TiN/TaN superlattices. *Surf. Coat. Technol.* **2014**, *254*, 21–27. [\[CrossRef\]](#)
26. Shin, C.-S.; Gall, D.; Desjardins, P.; Vailionis, A.; Kim, H.; Petrov, I.; Greene, J.E. Growth and physical properties of epitaxial metastable cubic TaN(001). *Appl. Phys. Lett.* **1999**, *75*, 3808–3810. [\[CrossRef\]](#)
27. Bader, R.F.W. *Atoms in Molecules: A Quantum Theory*; Clarendon Press: Oxford, UK, 1990; p. 458.
28. Dronskowski, R.; Bloechl, P.E. Crystal orbital Hamilton populations (COHP): Energy resolved visualization of chemical bonding in solids based on density-functional calculations. *J. Phys. Chem.* **1993**, *97*, 8617–8624. [\[CrossRef\]](#)
29. Deringer, V.L.; Tchougréeff, A.L.; Dronskowski, R. Crystal orbital Hamilton population (COHP) analysis as projected from plane-wave basis sets. *J. Phys. Chem. A* **2011**, *115*, 5461–5466. [\[CrossRef\]](#)
30. Maintz, S.; Deringer, V.L.; Tchougréeff, A.L.; Dronskowski, R. Analytic projection from plane-wave and PAW wavefunctions and application to chemical-bonding analysis in solids. *J. Comput. Chem.* **2013**, *34*, 2557–2567. [\[CrossRef\]](#)
31. Maintz, S.; Deringer, V.L.; Tchougréeff, A.L.; Dronskowski, R. LOBSTER: A tool to extract chemical bonding from plane-wave based DFT. *J. Comput. Chem.* **2016**, *37*, 1030–1035. [\[CrossRef\]](#)
32. Mastail, C.; David, M.; Nita, F.; Michel, A.; Abadias, G. Ti, Al and N adatom adsorption and diffusion on rocksalt cubic AlN (001) and (011) surfaces: Ab initio calculations. *Appl. Surf. Sci.* **2017**, *423*, 354–364. [\[CrossRef\]](#)
33. Holec, D.; Mayrhofer, P.H. Surface energies of AlN allotropes from first principles. *Scr. Mater.* **2012**, *67*, 760–762. [\[CrossRef\]](#) [\[PubMed\]](#)
34. Forslund, A.; Zhang, X.; Grabowski, B.; Shapeev, A.V.; Ruban, A.V. Ab initio simulations of the surface free energy of TiN(001). *Phys. Rev. B* **2021**, *103*, 195428. [\[CrossRef\]](#)
35. Gall, D.; Kodambaka, S.; Wall, M.A.; Petrov, I.; Greene, J.E. Pathways of atomistic processes on TiN(001) and (111) surfaces during film growth: An ab initio study. *J. Appl. Phys.* **2003**, *93*, 9086–9094. [\[CrossRef\]](#)
36. Siodmiak, M.; Govind, N.; Andzelm, J.; Tanpipat, N.; Frenking, G.; Korkin, A. Theoretical Study of Hydrogen Adsorption and Diffusion on TiN(100) Surface. *Phys. Status Solidi B* **2001**, *226*, 29–36. [\[CrossRef\]](#)
37. Lebeda, M.; Vlčák, P.; Veřtát, P.; Drahoukoupil, J. Ab-initio study of Surface energies and Structural Influence of vacancies in Titanium Nitride nanolayer. In Proceedings of the 12th International Conference on Nanomaterials—Research & Application, Brno, Czech Republic, 21–23 October 2020.
38. Sanyal, S.; Waghmar, U.V.; Ruud, J.A. Adsorption of water on TiN (1 0 0), (1 1 0) and (1 1 1) surfaces: A first-principles study. *Appl. Surf. Sci.* **2011**, *257*, 6462–6467. [\[CrossRef\]](#)
39. Tholander, C.; Alling, B.; Tasnádi, F.; Greene, J.E.; Hultman, L. Effect of Al substitution on Ti, Al, and N adatom dynamics on TiN(001), (011), and (111) surfaces. *Surf. Sci.* **2014**, *630*, 28–40. [\[CrossRef\]](#)
40. Moré, S.; Berndt, W.; Bradshaw, A.M.; Stumpf, R. Ordered phases of potassium on Pt{111}: Experiment and theory. *Phys. Rev. B* **1998**, *57*, 9246–9254. [\[CrossRef\]](#)
41. Lai, W.Z.; Xie, D.Q. First-Principles Study of K and Cs Adsorbed on Pd(111). *J. Phys. Chem. B* **2006**, *110*, 23904–23910. [\[CrossRef\]](#)
42. Marlo, M.; Milman, V. Density-functional study of bulk and surface properties of titanium nitride using different exchange-correlation functionals. *Phys. Rev. B* **2000**, *62*, 2899. [\[CrossRef\]](#)
43. Mehmood, F.; Pachter, R.; Murphy, N.R.; Johnson, W.E. Electronic and optical properties of titanium nitride bulk and surfaces from first principles calculations. *J. Appl. Phys.* **2015**, *118*, 195302. [\[CrossRef\]](#)
44. Barnard, A.S. Shape and Energetics of TiN Nanoparticles. *J. Comput. Theor. Nanosci.* **2004**, *1*, 334–339. [\[CrossRef\]](#)
45. Stampfl, C.; Freeman, A.J. Metallic to insulating nature of TaN_x: Role of Ta and N vacancies. *Phys. Rev. B* **2003**, *67*, 064108. [\[CrossRef\]](#)
46. Steinberg, S.; Dronskowski, R. The Crystal Orbital Hamilton Population (COHP) Method as a Tool to Visualize and Analyze Chemical Bonding in Intermetallic Compounds. *Crystals* **2018**, *8*, 225. [\[CrossRef\]](#)
47. Helmer, P.; Lind, H.; Dahlqvist, M.; Rosen, J. Investigation of out-of-plane ordered Ti₄MoSiB₂ from first principles. *J. Phys. Condens. Matter* **2022**, *34*, 185501. [\[CrossRef\]](#)
48. Tripathi, D.; Ray, P.; Singh, A.V.; Kishore, V.; Singh, S.L. Durability of Slippery Liquid-Infused Surfaces: Challenges and Advances. *Coatings* **2023**, *13*, 1095. [\[CrossRef\]](#)

Disclaimer/Publisher’s Note: The statements, opinions and data contained in all publications are solely those of the individual author(s) and contributor(s) and not of MDPI and/or the editor(s). MDPI and/or the editor(s) disclaim responsibility for any injury to people or property resulting from any ideas, methods, instructions or products referred to in the content.